POST-FLIGHT ANALYSES OF THE CRYSTALS FROM THE M0003-14 QUARTZ CRYSTAL MICROBALANCE EXPERIMENT

W.K.Stuckey and G. Radhakrishnan
The Aerospace Corporation
2350 East El Segundo Blvd.
El Segundo, CA 90245
Phone: 310/336-7389, FAX: 310/336-5846

D. Wallace
QCM Research
PO Box 277
Laguna Beach, CA 92652
Phone: 714/497-5748, FAX 714/497-7331

SUMMARY

Quartz Crystal Microbalances constructed by QCM Research were flown on the leading and trailing edges of LDEF as one of the sub-experiments of M0003. Response of the crystals coated with 150 Å of In_2O_3 was recorded during the first 424 days of the mission. A second QCM with crystals coated with 150 Å of ZnS was also flown but not monitored. After the flight, the QCMs were disassembled and analyzed in The Aerospace Corporation laboratories. The samples included the crystals from the leading and trailing edge samples of both types of coatings along with the reference crystals, which were inside the QCM housing. Analyses were performed by scanning electron microscopy, energy dispersive X-ray analyses, X-ray photoelectron spectroscopy, ion microprobe mass analysis, and reflectance spectroscopy in the infrared and UV/visible regions. The crystals are contaminated predominantly with silicone compounds. The contamination is higher on the leading edge than on the trailing edge and higher on the exposed crystals than on the reference crystals.

I. INTRODUCTION

Quartz crystal microbalances (QCMs) were flown on the Long Duration Exposure Facility (LDEF M0003-14) by QCM Research, Laguna Beach, California, as contamination monitors. This sub-experiment was one of 19 sub-experiments that comprised the M0003 experiment assembled by The Aerospace Corporation. The QCMs used 10-MHz quartz crystals with two types of coatings. One set of leading and trailing edge QCMs consisted of crystals with 9000Å of aluminum and aluminum oxide (Al + Al_2O_3), and a top layer of 150 Å of indium oxide (In_2O_3). The second set of crystals on the leading and trailing edges consisted of 9000 Å (Al + Al_2O_3) and a top layer of 150 Å zinc sulfide (ZnS). Each of the QCMs consists of a pair of crystals, one exposed to the environment and termed the "sense" crystal, and one that remained unexposed and, hence, termed the "reference" crystal. The beat frequency monitored between the "sense" and "reference" crystals represents the change in mass of the "sense" crystal as a result of exposure, relative to the unexposed "reference" crystal.

The QCM response was recorded for about 14 months, the lifetime of the data acquisition batteries. The crystals continued to be exposed to the Low Earth Orbit Environment on Row 9 on the leading edge of LDEF and Row 3 on the trailing edge for the entire LDEF mission, even though the response was no longer recorded. An analysis of the crystals was performed at The Aerospace Corporation after retrieval to deter-

mine the accumulated contamination deposition and the effects of exposure of the crystals to the space environment.

II. QUARTZ CRYSTAL MICROBALANCE DATA

On-orbit information was recorded by the Experiment Power and Data System (ref. 1) from various sensors located throughout the four experiment trays constituting the M0003 experiment. Special circuits were included to measure QCM frequency, which allowed monitoring the frequency of one set of the crystals during the data acquisition part of the mission. The crystals with the In_2O_3 coating were selected for the on-orbit data acquisition. Data were recorded in bursts lasting a period of 111.7 min (about one LDEF orbit). During this 111.7-min period, each data channel was scanned 32 times, producing a profile for the entire orbit. After the burst period, the data system rested for 93.16 h before the start of the next burst period. Data were taken in this manner until the end of the recording media was reached, 424 days after launch. The maxima and minima frequencies recorded for the leading and trailing edge QCMs during each period are shown in Fig. 1. The variation is due to the temperature response of the QCMs during each orbit. The variations in the maxima response curves are consistent with the temperature response variations due to the solar exposures. Note that the trailing edge QCM indicates a slight increase in weight during the 424-day data acquisition period while the leading edge shows an apparent weight loss.

III. ANALYSES OF QCM CRYSTALS

Post-flight analysis of the separate quartz crystals (QCs) constituting the QCMs has been performed at The Aerospace Corporation in an effort to determine the effects of the 69-month-long exposure on the surface composition of the crystals. The frequency and temperature response curves of the QCMs were measured by QCM Research, following which they were disassembled and then cleaned with acetone and hexane. The individual crystals were then brought to The Aerospace Corporation for analysis. The QCs are numbered 1-8 in the following sections, in correspondence with the numbering sequence in Table 1.

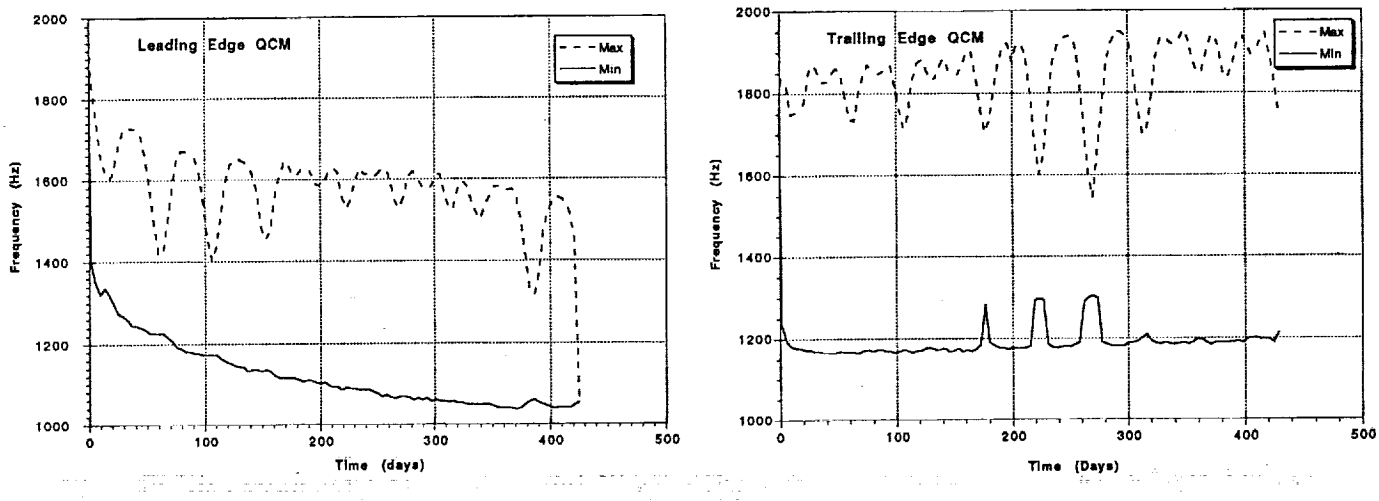

Figure 1. Quartz crystal microbalance data recorded on LDEF.

Table 1. Quartz Crystal Identification.

QC#	QCM Location	QCM#	Composition	LDEF Position
1	Sense	TP329	Al + Al_2O_3 (9000 Å) / In_2O_3 (150 Å)	Leading Edge, Active
2	Reference	TP329	Al + Al_2O_3 (9000 Å) / In_2O_3 (150 Å)	Leading Edge, Active
3	Sense	TP330	Al + Al_2O_3 (9000 Å) / ZnS (150 Å)	Leading Edge, Passive
4	Reference	TP330	Al + Al_2O_3 (9000 Å) / ZnS (150 Å)	Leading Edge, Passive
5	Sense	TP318	Al + Al_2O_3 (9000 Å) / In_2O_3 (150 Å)	Trailing Edge, Active
6	Reference	TP318	Al + Al_2O_3 (9000 Å) / In_2O_3 (150 Å)	Trailing Edge, Active
7	Sense	TP353	Al + Al_2O_3 (9000 Å) / ZnS (150 Å)	Trailing Edge, Passive
8	Reference	TP353	Al + Al_2O_3 (9000 Å) / ZnS (150 Å)	Trailing Edge, Passive

Table 2. Large Area EDAX Analyses at 5 kV with Sample Surface at Normal Incidence (4 mm x 5 mm), and with Sample Surface Inclined 60° (2 mm x 5 mm).

Sample	QC	Sample Orientation	Atomic %				
			In	Zn	Si	Al	S
In_2O_3 Leading Edge	Sense #1	0°	19	n.d.	2.9	79	n.d.
		60° tilt	22	n.d.	7.8	70	n.d.
	Ref. #2	0°	19	n.d.	n.d.	81	n.d.
		60° tilt	21	n.d.	7.9	71	n.d.
ZnS Leading Edge	Sense #3	0°	n.d.	2.2	2.6	94	1.3
		60° tilt	n.d.	2.9	5.5	87	4.2
	Ref.#4	0°	n.d.	4.2	5.0	83	7.5
		60° tilt	n.d.	5.6	5.2	75	14
In_2O_3 Trailing Edge	Sense #5	0°	21	n.d.	2.0	77	n.d.
		60° tilt	24	n.d.	1.3	75	n.d.
	Ref. #6	0°	20	n.d.	0.7	80	n.d.
		60° tilt	21	n.d.	4.0	75	n.d.
ZnS Trailing Edge	Sense #7	0°	n.d.	6.0	0.8	85	8.0
		60° tilt	n.d.	8.5	4.5	72	15
	Ref. #8	0°	n.d.	5.4	n.d.	86	8.4
		60° tilt	n.d.	7.4	7.9	69	16

A. SEM / EDAX Measurements

SEM photographs of all the crystals were obtained at magnifications of X10, X50, X1000, and X5000. More revealing are the large area EDAX measurements (spanning an area of 10 to 20 mm^2) shown in Table 2. Elements not detected are marked n.d. The detection of silicon (Si) with the probe beam at normal incidence to the sample at 5 kV suggests the presence of Si primarily as a contaminant on the surface of these crystals and to a lesser extent coming from the underlying quartz. To further enhance contributions of elements present on the surface and better identify contaminants on the surface of the crystals, data were taken with the sample tilted 60° with respect to the probe beam. As seen in Table 2, the 5-kV measurements performed with tilted samples confirm the presence of Si primarily as a contaminant on the surface. For the In_2O_3-coated crystals, on the leading edge, in both the sense and reference crystals 1 and 2, a significantly

higher concentration of Si (factor of 3 or more) is detected on the tilted sample relative to the untilted sample. It should also be pointed out that in both crystals, the levels of In detected in the tilted samples are just slightly higher than the corresponding untilted samples, while the levels of Al are lower on the tilted samples, suggesting that Al is a bulk component. The concentrations of In, Si, and Al are observed to be nearly equal on the sense and reference crystals on the leading edge. On the trailing edge samples 5 and 6, while the behavior of In and Al are quite similar to the leading edge counterparts 1 and 2, it can be seen that the detected levels of Si on the trailing edge are (i) not as high as on the leading edge and (ii) higher on the reference crystal 6 than on the sense crystal 5. This suggests that on the In_2O_3 samples, there is (i) higher surface contamination by Si on the leading edge crystals than on the trailing edge crystals, and (ii) on the trailing edge, a slightly higher contamination on the reference crystal than on the corresponding sense crystal. A comparison of Figs. 2 and 3 clearly shows the higher Si levels on the leading edge In_2O_3 crystals.

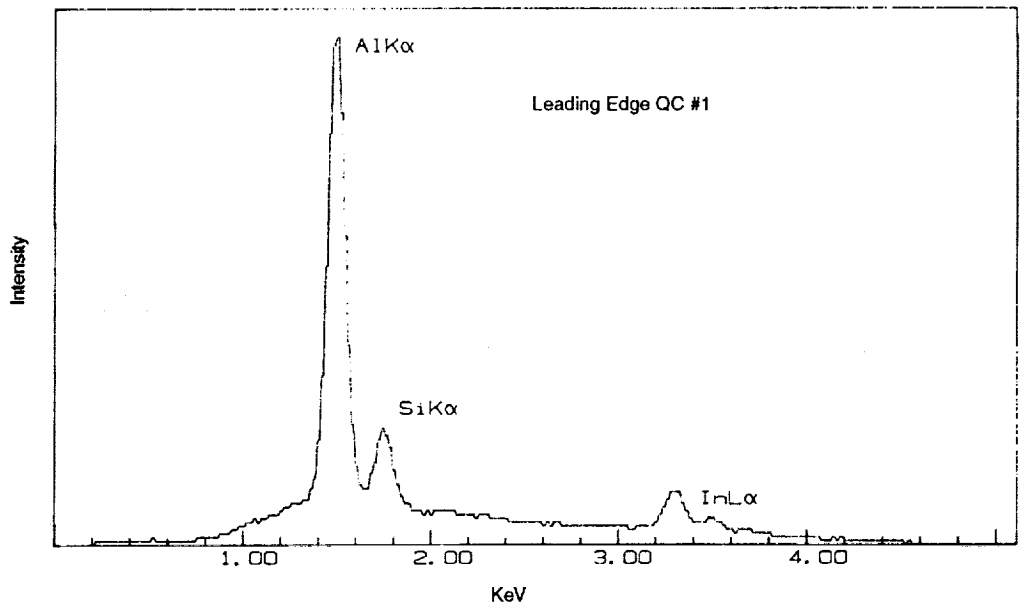

Figure 2. EDX Spectrum of Leading Edge In_2O_3 Crystal (QC #1)

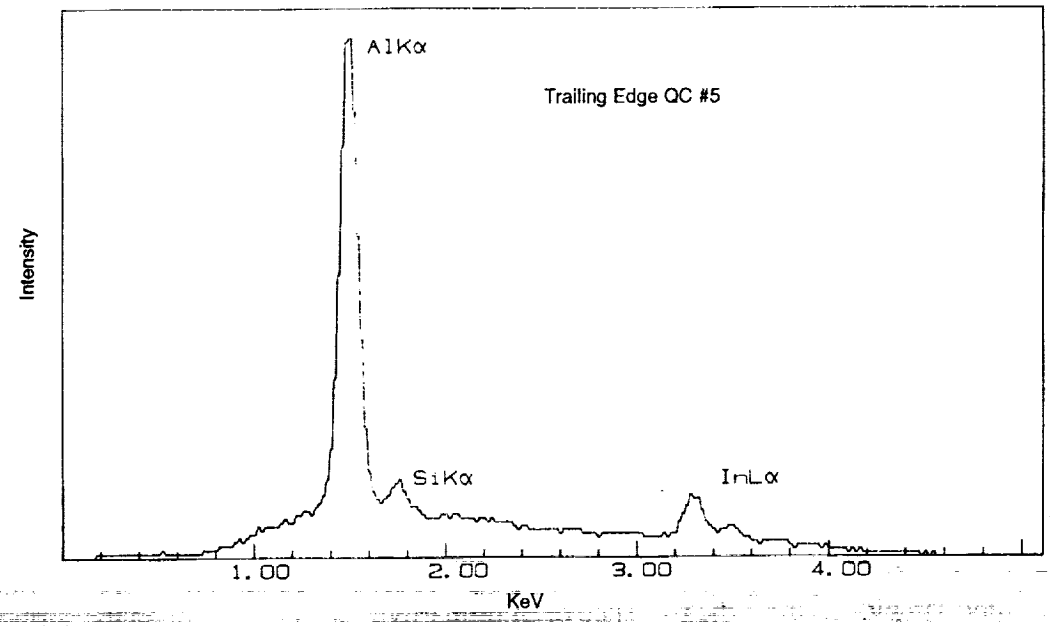

Figure 3. EDX Spectrum of Trailing Edge In_2O_3 Crystal (QC #5)

With the ZnS coated crystals, it is observed that on the leading edge, while the sense crystal 3 shows a factor of 3 higher Si when tilted, the reference crystal 4 shows no measurable difference in Si levels with tilt. On the trailing edge crystals 7 and 8, however, there appears to be significantly higher levels of Si on tilting the crystals. All four crystals show an increase in concentration of both Zn and S when tilted. While the increase in Zn is nearly the same in all four samples (~ 1.3), the concentration of S increases by a factor of ~3 in QC 3 and ~2 in QCs 4, 7, and 8. The results can be summarized as (i) higher Si contamination on the sense crystal on the leading edge than on the sense crystal on the trailing edge, but a higher Si contamination on the reference crystal on the trailing edge than on the leading edge, (ii) comparing sense crystal 3 with reference crystal 4 on the leading edge and with crystals 7 and 8 on the trailing edge, it is observed that although the increase in the Zn and S concentrations on tilting are comparable, the ZnS coating appears to have thinned in sense crystal 3, as indicated by considerably lower percentages of both Zn and S in QC 3 relative to QCs 4, 7, and 8. While these measurements were not performed before flight, all samples were deposited such that the coatings should have been identical.

B. XPS Analyses

The instrument used for analysis was a VG ESCALAB MK II. A Mg Kα X-ray source (hν = 1253.6 eV) was chosen for irradiation. Base pressure during analysis was approximately 5 x 10^{-} torr. Secondary electron imaging was used to align each crystal for XPS analysis to ensure that edge effects were minimized. The analysis on these crystals was performed as received, and the analysis area was approximately 4 mm x 5 mm. XPS analyses were conducted on all of the above crystals. XPS is a very surface sensitive technique, probing only about 100 Å of the outermost surface.

A comparison of leading edge crystals (1, 2, 3, and 4) vs trailing edge crystals (5, 6, 7, and 8) indicates that there is a higher percentage Si coverage on the leading edge. In addition, a comparison of the sense crystals vs the reference crystals indicates a higher percentage Si coverage on the sense crystals. The results are tabulated in Table 3 . A comparison of the XPS data and the 5-kV EDAX data reveals several interesting features. These are discussed below, taking pairs of sense and reference crystals one at a time on the leading and trailing edges.

Table 3. XPS analyses of QC surfaces (n.d. = not detected and tr = trace)

		Surface Mole % (Normalized)													
Sample	QC	C	O	Si	In	Sn	Zn	S	Pb	K	Na	N	Cl	Al	Ag
In_2O_3 Leading Edge	Sense #1	17	58	23	0.7	0.2	n.d.	0.1	n.d.	tr	0.3	0.8	tr	n.d.	n.d.
	Ref. #2	53	31	1.9	6.4	1.0	0.1	0.1	0.5	0.1	1.0	4.5	0.2	n.d.	n.d.
ZnS Leading Edge	Sense #3	48	35	10	n.d.	0.2	0.9	0.5	0.1	tr	0.4	3.5	0.1	1.4	n.d.
	Ref.#4	61	23	1.0	n.d.	0.2	2.0	5.5	0.3	tr	0.7	4.7	0.4	n.d.	1.2
In_2O_3 Trailing Edge	Sense #5	68	25	1.5	n.d.	0.3	n.d.	0.1	0.3	n.d.	0.1	4.7	0.2	0.4	n.d.
	Ref. #6	65	24	0.2	2.3	0.7	0.1	0.2	0.4	n.d.	0.1	6.3	0.1	n.d.	n.d.
ZnS Trailing Edge	Sense #7	67	25	2.3	n.d.	0.4	0.1	0.1	0.4	n.d.	0.1	4.5	0.3	n.d.	n.d.
	Ref. #8	68	20	n.d.	n.d.	0.3	1.4	3.9	0.3	tr	0.3	4.1	0.3	n.d.	0.6

QC 1 (Sense) and QC 2 (Reference): 150 Å In_2O_3 Coating; Leading Edge

In crystals 1 and 2, while EDAX measured nearly equal percentages of In (19% or ~22% when tilted), XPS analyses indicated nearly an order of magnitude lower value of In in the sense crystal 1 (0.7) compared to the reference crystal 2 (6.4). XPS also indicated a much higher Si coverage on the sense crystal (23) than on the reference crystal (1.9), also illustrated in Figs. 4 and 5. The data suggest that in crystal 1, surface

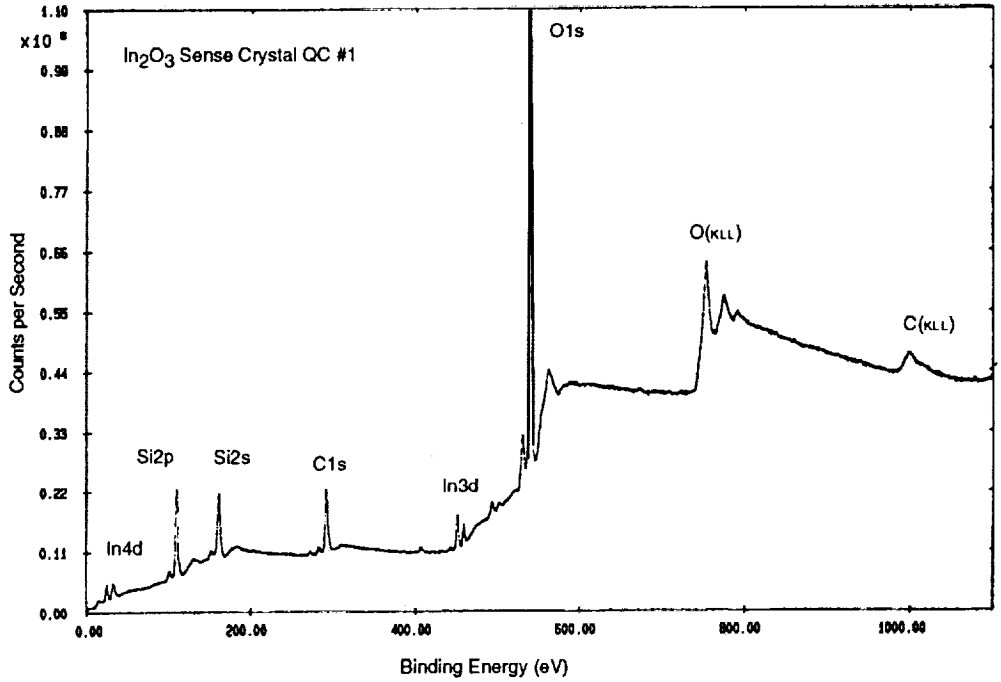

Figure 4. XPS Spectrum of Leading Edge In_2O_3 Sense Crystal (QC #1)

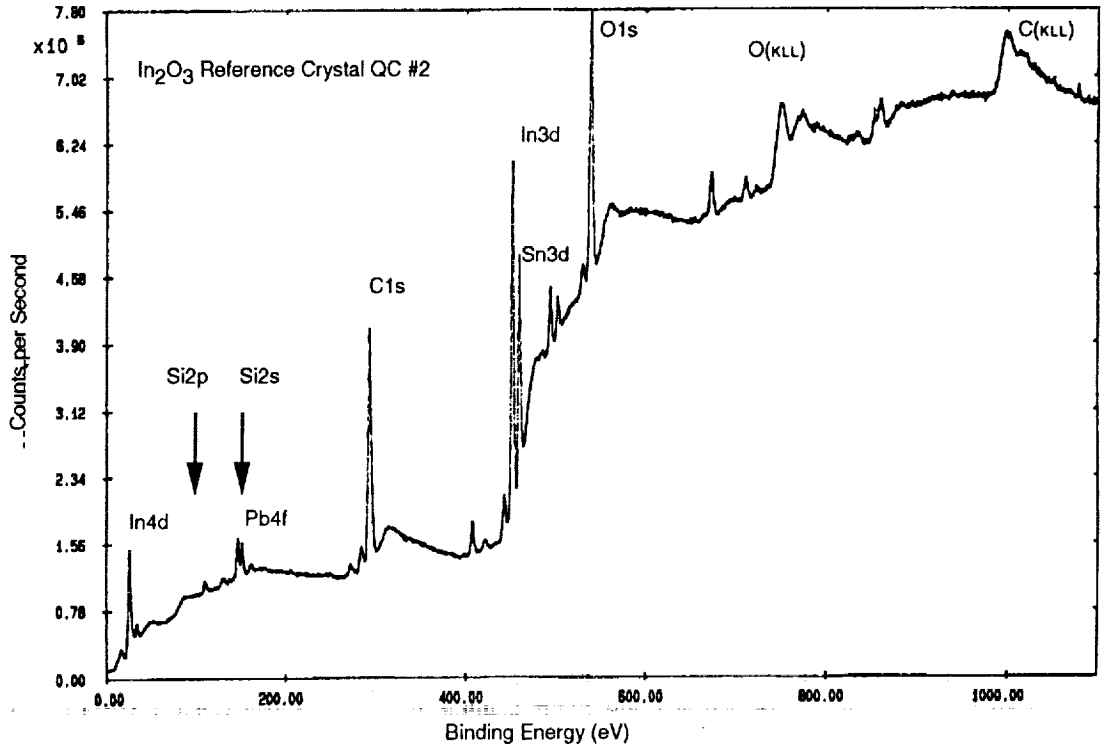

Figure 5. XPS Spectrum of Leading Edge In_2O_3 Reference Crystal (QC #2)

contamination and coverage of the In_2O_3 layer by Si could most likely be the cause of the lower In content as detected by XPS. While these results are in qualitative agreement with the normal incidence EDAX data, the tilted EDAX data do not indicate a difference in Si between QC 1 and QC 2.

QC 5 (Sense) and QC 6 (Reference) : 150 Å In_2O_3 Coating; Trailing Edge

Similar to the leading edge pair 1 and 2, EDAX measurements indicate nearly equal percentages of In in the sense and reference pairs 5 and 6 on the trailing edges (~21% and an average of ~22 % when tilted). In is not detected on the sense crystal 5 by XPS analysis, while it is detected in the reference crystal 6 (2.3). This appears to be consistent with the fact that a factor of 7 higher Si concentration is measured on the sense crystal 5 by XPS, in comparison to the reference 6. Again, the normal incidence EDAX results are in qualitative agreement with the XPS results, indicating a factor of 3 higher Si concentration on the sense crystal 5 relative to reference 6. However, the tilted EDAX measurements show a reverse trend.

QC 3 (Sense) and QC 4 (Reference) : 150 Å ZnS Coating; Leading Edge

In this pair of crystals, both XPS and EDAX measurements are in agreement with respect to the nearly 50% lower Zn concentration on the sense crystal 3 compared to the reference crystal 4. While XPS measures a much lower S concentration on QC 5 than on QC 6 (factor of 11), EDAX results show a smaller difference (~factor of 5). There is a discrepancy in the amounts of Si detected by these two methods, whereby XPS indicates a 10-to-1 ratio of Si between the sense and reference, while normal incidence EDAX indicates a reverse trend with a 50% higher Si concentration in the reference sample, and tilted EDAX shows no measurable difference.

QC 7 (Sense) and QC 8 (Reference) : 150 Å ZnS Coating; Trailing Edge

In this case, EDAX measures nearly equal concentrations of Zn (~6% and ~8% when tilted) as well as of S (~8% and ~16% when tilted) on the sense and reference crystals. XPS measures significantly lower concentrations of both Zn and S in the sense crystal (Zn: 0.1, S: 0.1) than in the reference crystal (Zn: 1.4, S: 3.9). With both XPS and normal incidence EDAX, Si is only detected on the sense crystal, not on the reference crystal. However, with tilted samples, a reverse trend is observed, and more Si is detected on the reference crystal than on the sense crystal. The XPS data are once again suggestive of Si coverage on the sense crystal, which will attenuate the amount of Zn detected.

C. SIMS Analyses and Depth Profiling

To gather more information on the Si contamination and coverage issues, depth profiles using the secondary ion mass spectrometry (SIMS) technique were made on each of the QCM samples. A thin film of carbon was first deposited on the surface of all the samples to minimize charging, and the analyses were performed by sputter etching through the carbon film. This technique worked well on the In_2O_3-coated crystals. It did not work as well on the ZnS-coated crystals.

Depth profiles and elemental analyses were made with an Applied Research Laboratories (ARL) ion microprobe mass analyzer (IMMA) using a 1 nA primary beam of oxygen ($^{18}O_2^+$) ions accelerated to 4.5 kV and focused to approximately 15 μm in diameter. The primary beam was rastered over an area measuring 100 μm x 80 μm, and data was collected from the center utilizing an electronic aperture to minimize

contribution from the crater edges. The IMMA detects secondary ions emitted from the surface in the area probed by the primary ion beam. The depth profiles were made following elements of each of (a) the contaminants (Si, K, Mg), (b) the coating (In, Zn), and (c) the substrate (Al).

Silicon, presumably from silicone, was detected on the surfaces of QCs 1, 3, 5, and 7. In addition to the elements given in Table 4, a significant Pb peak (Pb/Zn = 0.381) was detected on reference QC 8. The K appears to have been deposited with the Si, and its origin is unknown at this time. The source of the Mg detected is also unknown. Table 4 gives the ratio of the major ions of these elements detected at the surface of the coatings with respect to an element of the coating. The ratios are the peak level of a contaminant element ion vs the peak level of a coating element ion. A survey of the table shows that the Si+ intensity (a) is approximately 1 to 2 orders of magnitude higher on the sense crystals compared to the reference crystals, and (b) appears to be approximately an order of magnitude higher on the leading edge sense crystals compared to the trailing edge sense crystals.

Table 4. Ratios of Elements at QC Surfaces detected by SIMS Analysis

Sample	QC	Ion Ratios Mg^+/In^+	Si^+/In^+	K^+/In^+
In_2O_3 Leading Edge	Sense #1	0.058	0.27	0.094
	Ref. #2	0.00060	0.0010	0.019
In_2O_3 Trailing Edge	Sense #5	0.0067	0.036	0.31
	Ref.#6	0.0012	0.0015	0.014
		Mg^+/Zn^+	Si^+/Zn^+	K^+/Zn^+
ZnS Leading Edge	Sense #3	0.43	63	60
	Ref. #4	0.13	0.41	5.1
ZnS Trailing Edge	Sense #7	0.17	6.8	25
	Ref. #8	0.35	0.41	18

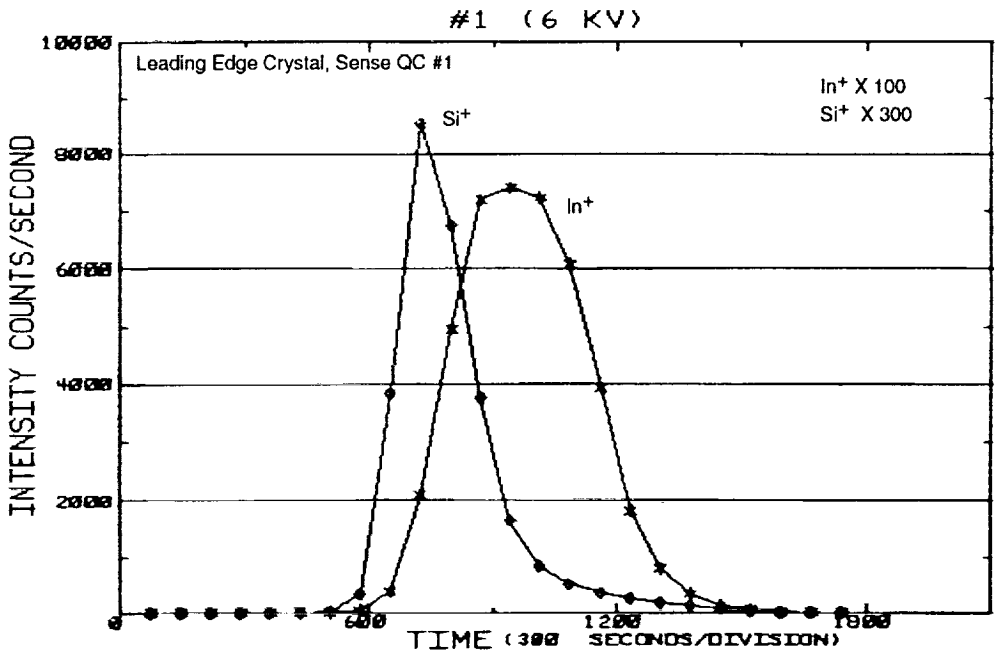

Figure 6. SIMS depth profiles on Si^+ and In^+ (leading edge, sense crystal, #1).

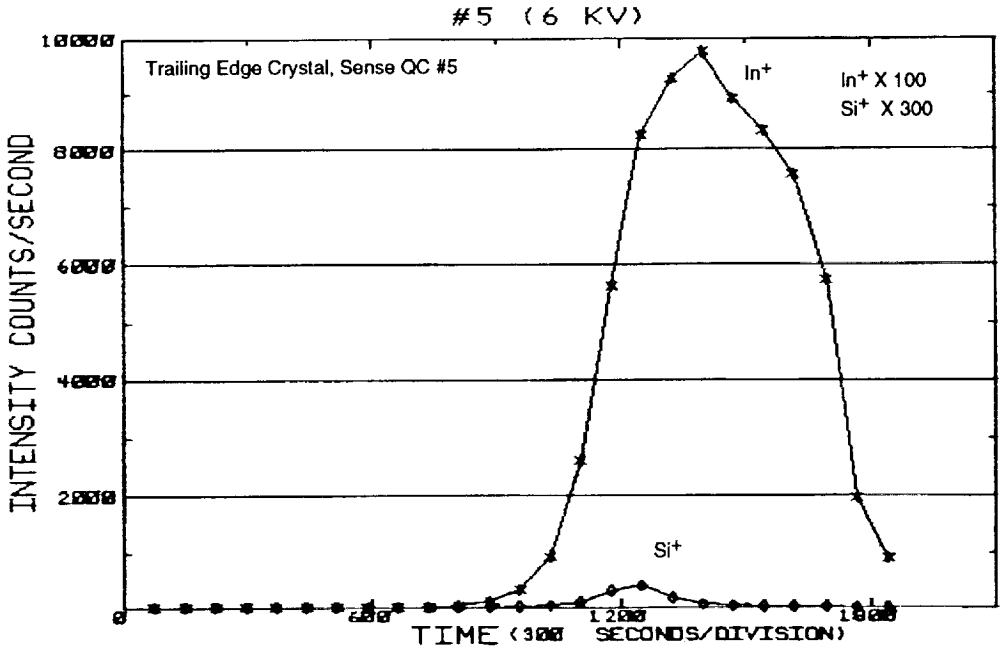

Figure 7. SIMS depth profiles on Si^+ and In^+ (trailing edge, sense crystal, #5).

deposited on the surface prior to analysis. On the sense crystal 1, a layer of Si occurs above the In_2O_3 layer. On the reference crystal 2, there is no distinct indication of Si coverage of the In_2O_3 layer. The presence of a significantly smaller Si layer above the In_2O_3 layer is detected on the sense crystal 5 in Figure 7, while on the reference crystal 6, Si is not present on the surface. Similar results are obtained from the ZnS-coated crystals although interpretation is hindered by charging of the sample upon reaching the ZnS layer.

D. FTIR Measurements

Infrared spectrometric analysis was performed with a Nicolet MX-1 Fourier Transform Infrared (FTIR) spectrometer, using the specular reflectance technique. Infrared radiation in the region 4000 to 400 cm^{-1} was obtained from a Globular Source. The beam was 5 mm in diameter at the sample. One hundred and twenty eight scans were taken for each sample at 3 to 4 seconds per scan with a resolution of 2 cm-1. Infrared spectroscopy is a surface-sensitive technique with a probing depth of < 0.5 μm. The FTIR spectra of the leading and trailing edge crystals are shown in Figs. 8 and 9. Important qualitative information may be derived from these measurements, and the results are summarized below.

An absorption characteristic of the Si-O stretching vibration (refs. 2 and 3) is observed on the leading edge sense crystals 1 and 3 at 1061 cm^{-1}. The most noticeable observation about these spectra is the absence of absorption at 1061 cm^{-1} on the leading edge reference crystals 2 and 4, as well as on all the trailing edge crystals 5 through 8. Since we know from the other measurements that Si is indeed present on the surface of the sense crystals on both the leading and trailing edges, results from the FTIR spectra must be interpreted as a measure of the relative concentrations of Si on the leading vs the trailing edges, as well as sense vs reference crystals, scaled by the sensitivity of this measurement.

Other absorptions due to C-H, C=O, and C=C stretching vibrations and C-H deformations were observed in both the leading and trailing edge crystals at approximately the same frequencies. All the crystals indicate the presence of C-H vibrations (refs. 2 through 4) in the range 2900 to 2500 cm^{-1}. In QC 3, there is

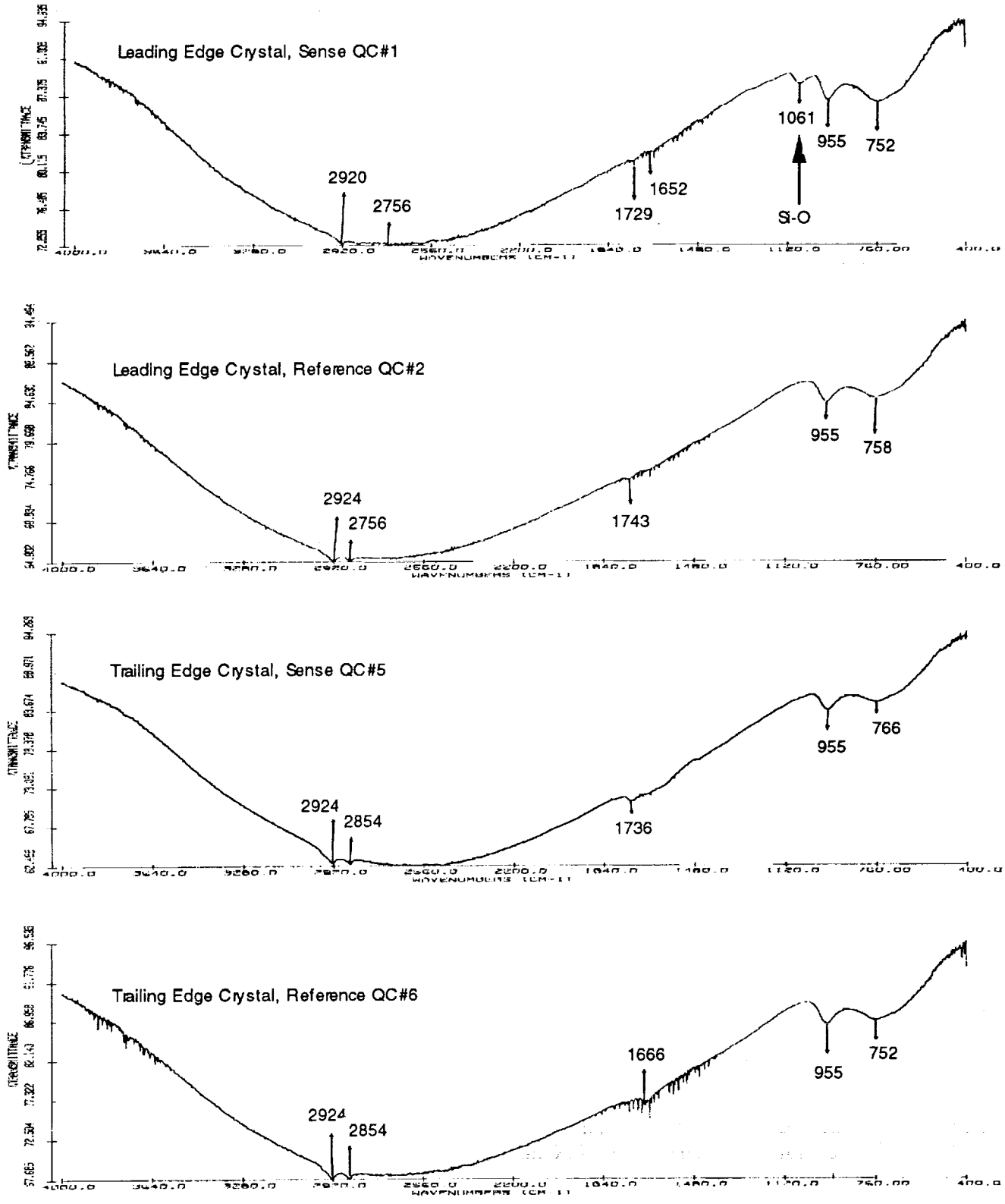

Figure 8. FTIR spectra of In_2O_3 crystals.

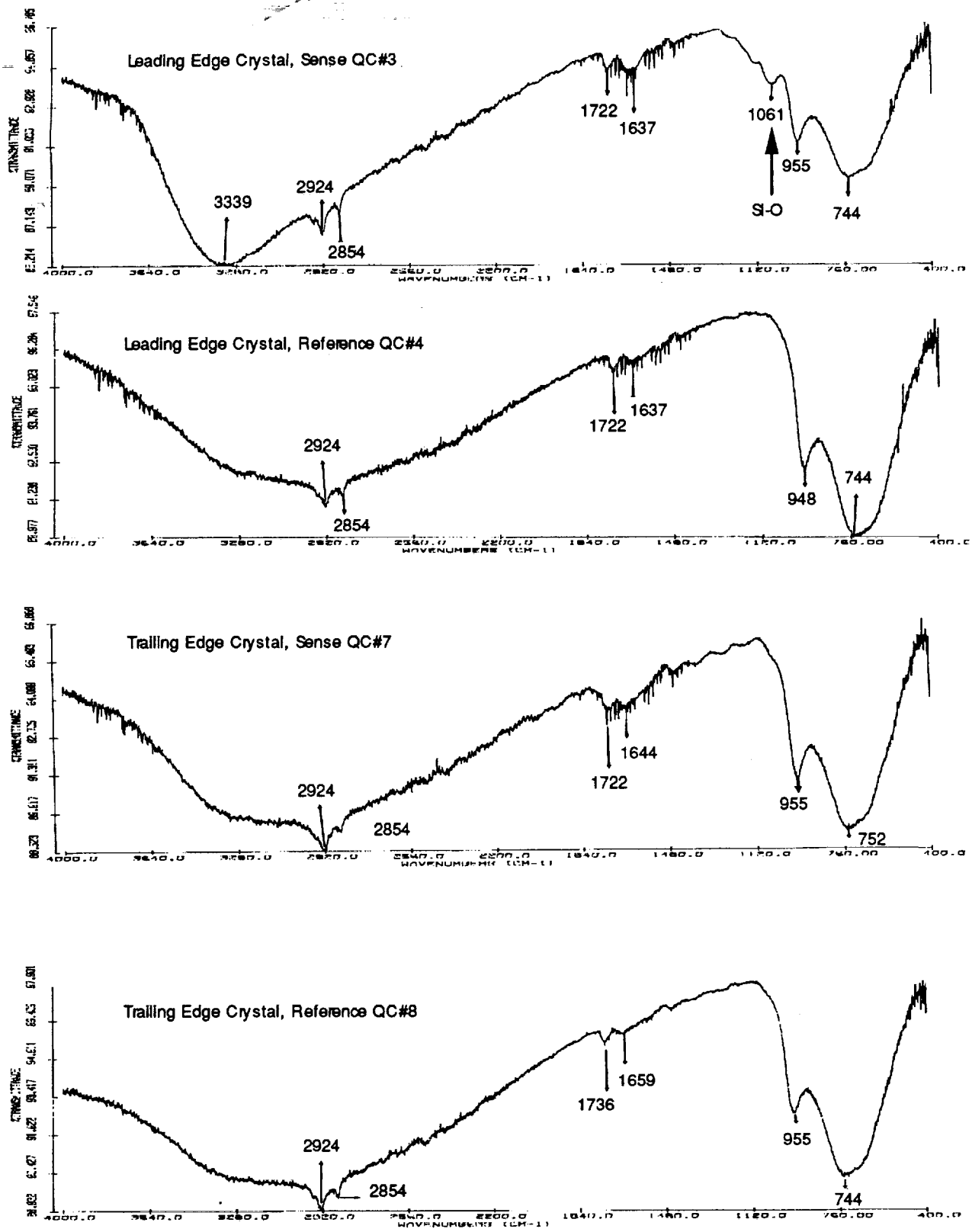

Figure 9. FTIR spectra of ZnS crystals.

strong absorption at 3339 cm^{-1}, which is due to the O-H stretch from water or alcohols on the surface.(ref. 4) A weak absorption at ~1740 cm^{-1}, seen in crystals 3, 4, 5,7, and 8 with varying intensities, is due to a carbonyl C=O group on the surface (ref. 4), while the most likely assignment of another weak absorption at ~ 1640 cm^{-1} seen in crystals 3, 4, 6, 7, and 8 is the C=C stretch from unsaturated hydrocarbons (ref. 4). An absorption at 955 cm^{-1} appears fairly consistently at the same position in all crystals with the exception of sample 4 where this peak is shifted to 948 cm^{-1}. Although the assignment of the absorption at 955 cm^{-1} remains ambiguous at the present time, it is most likely due to C-H deformations from alkenes (ref. 4). Other likely causes for this absorption could be the symmetric and asymmetric bends from SiH_3 or an Si-O-R (aromatic) stretching vibration. Shifts in the Si-O stretching vibrations, which generally occur in the range 1110 to 1000 cm^{-1}, from either Si-O-R (aliphatic) or Si-O-Si, may be alternative explanations (refs. 2 through 4). An absorption that generally appears in the range 760 to 740 cm^{-1} in both the leading and trailing edge crystals is found to be always shifted to higher frequencies in the sense crystals compared to the corresponding reference crystals. The most likely assignment of this absorption is the Al-O stretch (ref. 3) from the aluminum oxide layer present in all the crystals. C-H deformations due to alkanes (ref. 4) could also contribute to absorption at this frequency. Changes in local environment, especially on the sense crystals, could account for the shifts in the position of this peak.

E. Reflectance Measurements

Uncorrected diffuse reflectance was measured as a function of wavelength for each pair of sense-reference crystals on the leading and trailing edges. A Perkin Elmer Lambda-9 spectrophotometer was used for measuring the reflectance of the crystals. The light source was a deuterium lamp for the spectral range 319 nm to 250 nm. A halogen lamp was used for visible and infrared wavelengths longer than 300 nm. The reflected beam was collected by a lead sulfide detector for the infrared and a photomultiplier tube for the visible range. The data are given in Figs. 10 through 13. It should be pointed out that due to

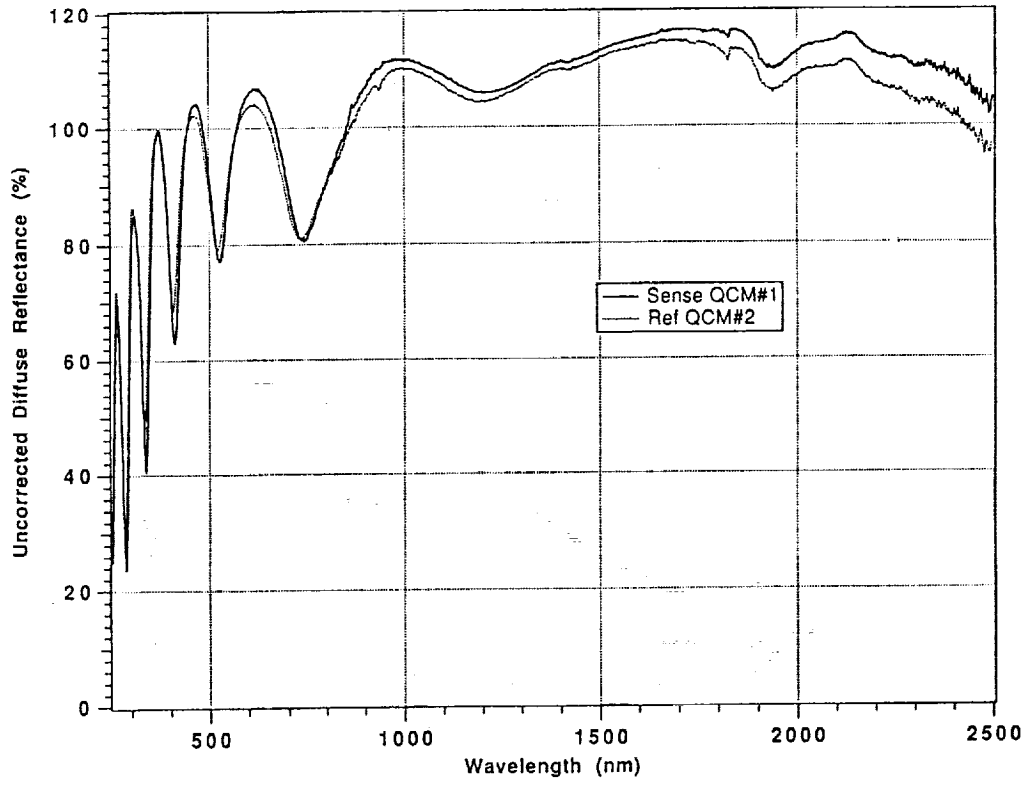

Figure 10. Diffuse reflectance spectra of leading edge crystals 1 and 2.

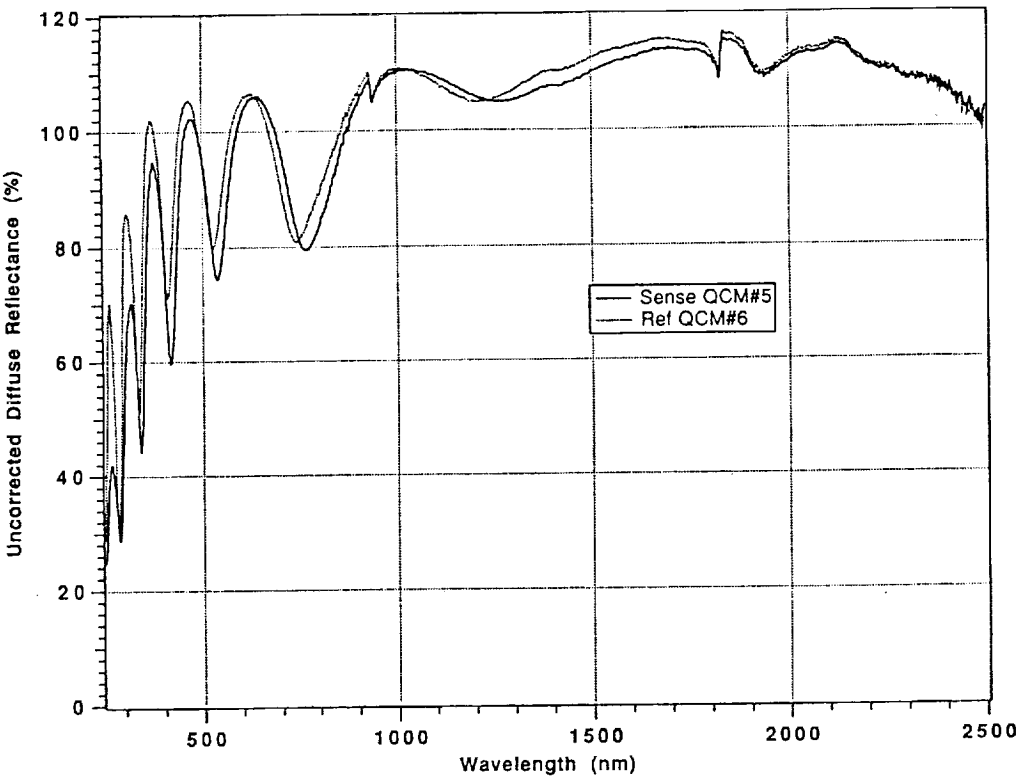

Figure 11. Diffuse reflectance spectra of leading edge crystals 3 and 4.

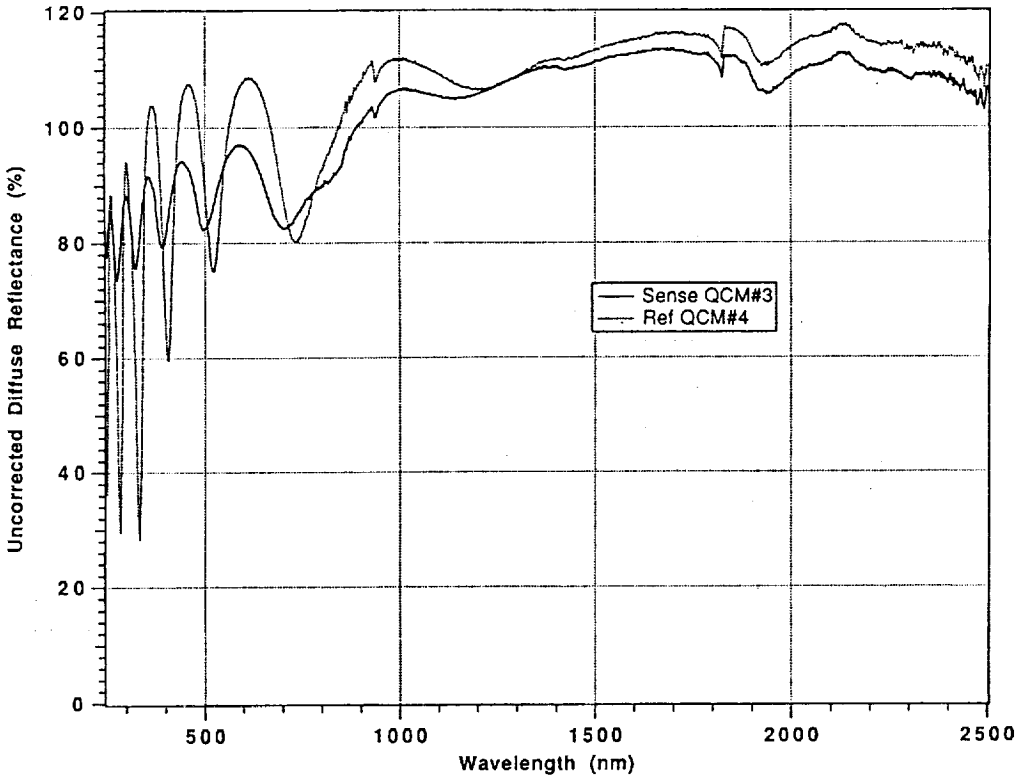

Figure 12. Diffuse reflectance spectra of trailing edge crystals 5 and 6.

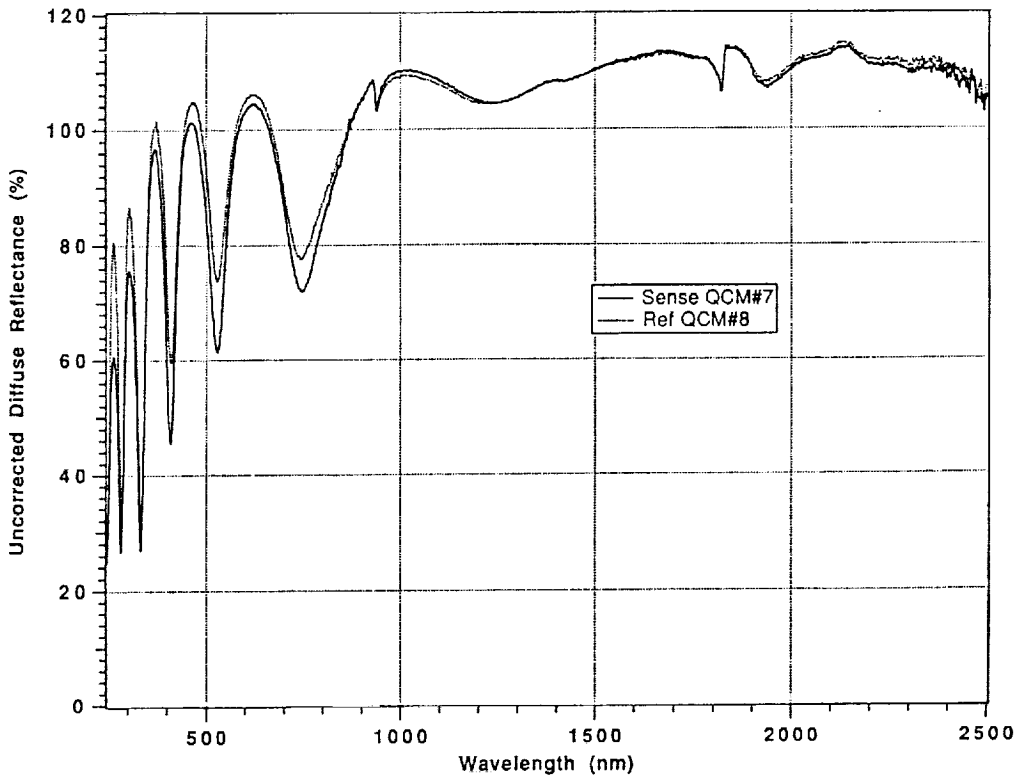

Figure 13. Diffuse reflectance spectra of trailing edge crystals 7 and 8.

a specially constructed experimental arrangement used to mount the crystals in the spectrophotometer, the reflectance data could not be normalized. Hence, they are plotted as uncorrected diffuse reflectance in arbitrary units, and it is only meaningful to compare relative values within each pair of crystals rather than the absolute values.

For all the crystals, it can be seen that with increasing wavelength, there is an increase in the corresponding average reflectance. In addition, it is seen that all the crystals also display thickness interference patterns in their reflectances. While the modulation amplitudes in crystals 1 and 2 are nearly identical, differences in modulation between QCs 5 and 6, and QCs 7 and 8 fall within a wide range of 2 to 20% in the wavelength range 2000 to 5000 Å. The most striking differences are observed with the pair 3, 4, where it is seen that the modulation amplitude in crystal 3 is significantly lower (by 10 to 50%) over the entire wavelength range (2000 to 10000 Å) than that of the reference crystal 4. On observing the positions of the wavelength maxima and minima in the interference patterns in each of the sense-reference crystal pairs, we see they appear to be negligibly shifted with respect to each other as well as with respect to the other crystal pairs, and are not large enough to result in significantly different values for the product (n x d), where n is the refractive index of the film, and d is the film thicknesses. In addition, the range of wavelengths at which these interferences are observed (2000 to 12000 Å) is so large that a 150 Å top layer either of In_2O_3 or ZnS cannot be responsible for the interferences, which are more likely due to the underlying Al/Al_2O_3 layer. A likely explanation for the observed behavior is that surface roughness can cause an increased scattering, which, in turn, can dampen the modulated amplitude of the reflected wave. In particular, EDAX analyses of the tilted samples reveal that QC 3 shows an overall thinning of the top ZnS layer, and particularly shows a reduction in the concentration of zinc present on the surface. This could result in scattering by sulfur particles or other contaminants on the surface and an overall damping of the modulated amplitude.

V. CONCLUSIONS

Silicon is the key contaminant identified on the surface of all the crystals. This conclusion is common to each of the analytical techniques employed, namely EDAX, XPS, SIMS, and FTIR. A second general conclusion supported by all these techniques is that the level of Si contamination is found to be higher on the leading edge than on the trailing edge, by about an order of magnitude. In addition, contaminants such as Mg, Ca, K, Na, Ag, Cl, Sn, and Pb have been detected on several of the crystals.

FTIR measurements detect a characteristic Si-O stretching vibration at approximately 1060 cm^{-1} only on the leading edge sense crystals, QC 1 and QC 3, which is consistent with the higher Si coverages observed on these crystals by XPS and SIMS. Reflectance measurements display modulations due to thickness interferences, with a significant damping on QC 3, which could be strongly related to the rather significant reduction of ZnS on the surface of this crystal and scattering caused by particulates or other contaminants on the surface. There were no surface compositional characteristics, which might explain the differences in frequency vs temperature curves observed on the trailing-edge QCMs after the LDEF flight.

Although all of the analytical techniques described above agree that Si, presumably from silicone, is the major contaminant on the QCs, the sources of silicone have not been unequivocally identified. There are, however, several likely candidates. Among these are the Z306 black paint in the interior of the spacecraft, silicone contaminant films on the surface of some trays prior to launch, silicone RTVs that were used to stabilize some components with respect to launch vibration, and tray cover gaskets. The relative contribution of all these sources has not been determined. In addition, while both ultraviolet radiation and atomic oxygen have been considered key factors responsible for the contamination, their relative roles, as well as the exact mechanism of contaminant production and deposition, are yet to be resolved.

ACKNOWLEDGEMENTS

The experimental contributions and useful discussions with John Coggi, Carol Hemminger, Nicholas Marquez, Mike Meshishnek, Nathan Presser, Barry Sinsheimer, Dave Sutton, Gloria To, and Joe Uht are gratefully acknowledged.

REFERENCES

1. "Long Duration Exposure Facility Experiment M0003 Deintegration/ Findings and Impacts" M.J. Meshishnek, S.R. Gyetvay, and C.H. Jaggers, Ist LDEF Post Retrieval Symposium, NASA CP-**3134**, Part 2, p. 1073–1107, Jan. 1992.
2. *Spectrometric Identification of Organic Compounds*, R.M. Silverstein, G.C. Bassler, and T.R. Morrill, John Wiley NY (1974).
3. *Infrared Spectra of Organic Compounds*, R.A. Nyquist and R.O. Kagel, Academic Press NY (1971).
4. *Introduction to Practical Infrared Spectroscopy*, A.D. Cross, Butterworths Publications, London (1960).